DOI: 10.1002/ejic.200700140

Synthesis, Upconversion Luminescence and Magnetic Properties of New Lanthanide–Organic Frameworks with $(4^3)_2(4^6,6^6,8^3)$ Topology

Danfeng Weng,[a] Xiangjun Zheng,*[a] Xiaobo Chen,[b] Licun Li,[c] and Linpei Jin*[a]

Keywords: Lanthanide–organic frameworks / Codoped coordination polymers / Upconversion properties / Magnetic properties

The synthesis and crystal structures of three new lanthanide–organic frameworks $[Ln(pza)(OH)(H_2O)]_n$ (Ln = Y(**1**), Er(**2**), Yb(**3**); H_2pza = 2,3-pyrazinedicarboxylic acid) with helical chains and novel 2D $(4^3)_2(4^6,6^6,8^3)$ topology are reported. The topology is obtained by simplifying the dinuclear metal core as a six-connected node and the ligand as a three-connected linker. The upconversion property measurement gives green and red emissions coming from two-photon excitation of Y: Er, Yb codoped coordination polymer and arising from Er^{III} transitions of $^4S_{3/2}/^2H_{11/2}\rightarrow{}^4I_{15/2}$ and $^4F_{9/2}\rightarrow{}^4I_{15/2}$. The magnetic properties of complexes **2** and **3** are also studied.

Introduction

The synthesis of metal–organic frameworks (MOFs) is an area of chemistry that has undergone a dramatic advance over recent years. Concerted efforts have been focused on exploiting the synthetic strategies at a level of framework design, with an impetus for illumination of structure–property relationships and an aim at certain properties and possible applications.[1] Various intriguing architectures and novel topologies have been reported,[2] among which the helical coordination polymers attracted special interests.[1f,1g,2d–g] These new materials with exploitable properties like microporosity,[3] chirality,[4] nonlinear optics,[2a,5] magnetism,[4d,6] etc. broaden the potential applications in gas storage and separation, catalysis, information storage and so on. Meanwhile, the multifunctional properties and potential applications of MOFs have gradually received more and more attention.[7] As for lanthanide–organic frameworks, complexes of Eu^{III} and Tb^{III}, which show luminescence in the visible region, are the most frequently employed, and their luminescence properties are extensively investigated.[8] To date, lanthanide upconversion phosphors which emit higher-energy photons when excited by lower-energy photons have attracted a great deal of interest, while the upconversion of lanthanide coordination polymers is less studied.[9] Recently, we have synthesized three new lanthanide–organic frameworks $[Ln(pza)(OH)(H_2O)]_n$ (Ln = Y(**1**), Er(**2**), Yb(**3**); H_2pza = 2,3-pyrazinedicarboxylic acid), which possess a novel $(4^3)_2(4^6,6^6,8^3)$ topology and multifunctional properties. The magnetic properties of complexes **2** and **3** and the upconversion properties of the codoped lanthanide (Y: Er, Yb) coordination polymers are investigated.

Results and Discussion

Structural Description

An X-ray diffraction study reveals that compound **1** adopts a layered, two-dimensional structure consisting of centrosymmetric $Y_2(\mu_2\text{-OH})_2$ units in which two μ_2-OH groups bridge two Y atoms with a Y···Y distance of 3.636 Å. The seven-coordinate environment around each Y centre is completed by two O atoms of two hydroxy groups, two O atoms from two pza ligands, one O atom and one N atom of a chelating pza ligand, and one O atom from one water molecule (see Figure 1). The pza ligand adopts a

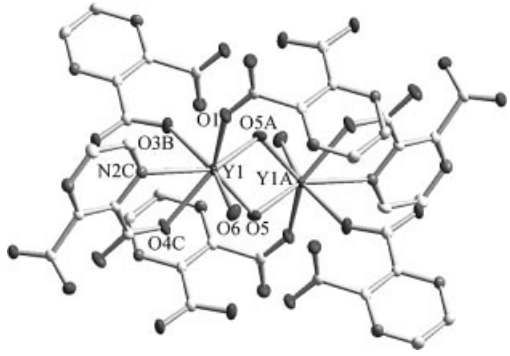

Figure 1. View of the dinuclear unit in complex **1** with ellipsoids drawn at the 50% probability level. All hydrogen atoms are omitted for clarity.

[a] Department of Chemistry, Beijing Normal University, Beijing 100875, P. R. China
Fax: +86-10-58802075
E-mail: lpjin@bnu.edu.cn
[b] Analytical and Testing Center, Beijing Normal University, Beijing 100875, P. R. China
[c] Department of Chemistry, Nankai University, Tianjin 300071, P. R. China

tetradentate coordination mode (Scheme 1). Selected bond lengths and bond angles of **1** are listed in Table 1.

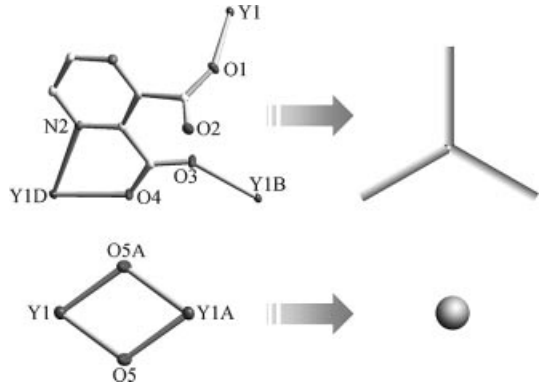

Scheme 1. Coordination mode of the pza ligand and topological simplification of the metal dinuclear unit and ligand.

The dinuclear $Y_2(\mu_2\text{-}OH)_2$ clusters bridged by pza ligands give rise to a neutral 2D grid extended in the (100) plane. Suitable nodes should be defined in order to analyze the network. In this complex, every $Y_2(\mu_2\text{-}OH)_2$ core is connected through six carboxylate groups from six pza ligands, in which there are two chelating N and O atom linkages simplified as monodentate linkers. Thus, the $Y_2(\mu_2\text{-}OH)_2$ core can be regarded as a six-connected node. And the pza ligand can be considered as a three-connected linker as shown in Scheme 1.

When viewed along the *b* axis, outer layers consisting of pza ligands and the dinuclear metal core layer that is embedded inside can be observed. Taking one surface of the pza ligand layer and the metal layer into consideration, the structure can be best described as a 2D network with a (6^3) topology (see Figure 2a). Further investigation of the whole 2D grid implies that two (6^3) topological structures arranged alternately are interweaved by metal nodes. There are six four-membered rings, six six-membered rings and three eight-membered rings around the six-connected metal node, while the three-connected linker is surrounded by three four-membered rings. Because the six-connected nodes and three-connected linkers are arranged in a ratio of $Y_2(OH)_2$/pza = 1:2, the short Schläfli symbol of the topology can be expressed as $(4^3)_2(4^6,6^6,8^3)$ (Figure 2b). The topological study for complex **1** was performed with TOPOS.[10] Furthermore, a supramolecular 3D framework can be built up from the 2D lanthanide–organic framework via hydrogen bonds [O6···N1E, 2.960(4) Å] and the π–π stacking of pyrazine rings with a calculated face-to-face distance of 3.261 Å (Figure 2a).

Another interesting feature of complex **1** is its single-helical chains (Figure 2c). The Y atoms are linked into an extended chain through the O5 atom from μ_2-OH and O1-, O3- carboxylate groups of the pza ligands. The repeating unit can be described as $(–Y1–O1–pza–O3–Y1B–O5B–)_n$, and the pitch of the helix running along the *b* axis is the same as its length (6.125 Å). It is worth noting that the chi-

Table 1. Selected bond lengths and bond angles of complexes **1**, **2** and **3** /Å [°].

Complex **1**[a]		Complex **2**[b]		Complex **3**[b]	
Y1–O5	2.193(2)	Er1–O5	2.180(3)	Yb1–O5	2.174(5)
Y1–O5#1	2.221(2)	Er1–O5#1	2.226(3)	Yb1–O5#1	2.196(5)
Y1–O1	2.268(2)	Er1–O4#2	2.266(4)	Yb1–O4#2	2.258(6)
Y1–O3#2	2.306(2)	Er1–O1	2.292(4)	Yb1–O1	2.283(6)
Y1–O4#3	2.325(2)	Er1–O2#3	2.312(3)	Yb1–O2#3	2.285(5)
Y1–O6	2.338(2)	Er1–O6	2.324(4)	Yb1–O6	2.313(5)
Y1–N2#3	2.586(2)	Er1–N2#3	2.566(4)	Yb1–N2#3	2.548(7)
O5–Y1–O5#1	69.0(1)	O5–Er1–O5#1	69.3(1)	O5–Yb1–O5#1	69.0(2)
O5–Y1–O1	133.5(1)	O5–Er1–O4#2	134.2(1)	O5–Yb1–O4#2	133.6(2)
O5#1–Y1–O1	82.2(1)	O5#1–Er1–O4#2	82.3(1)	O5#1–Yb1–O4#2	82.4(2)
O5–Y1–O3#2	117.9(1)	O5–Er1–O1	118.0(1)	O5–Yb1–O1	119.0(2)
O5#1–Y1–O3#2	79.4(1)	O5#1–Er1–O1	79.3(1)	O5#1–Yb1–O1	79.2(2)
O1–Y1–O3#2	90.3(1)	O4#2–Er1–O1	89.6(1)	O4#2–Yb1–O1	88.8(2)
O5–Y1–O4#3	78.0(1)	O5–Er1–O2#3	77.4(1)	O5–Yb1–O2#3	77.8(2)
O5#1–Y1–O4#3	133.3(1)	O5#1–Er1–O2#3	132.9(1)	O5#1–Yb1–O2#3	132.3(2)
O1–Y1–O4#3	143.2(1)	O4#2–Er1–O2#3	143.5(1)	O4#2–Yb1–O2#3	143.7(2)
O3#2–Y1–O4#3	88.3(1)	O1–Er1–O2#3	88.4(1)	O1–Yb1–O2#3	88.4(2)
O5–Y1–O6	82.5(1)	O5–Er1–O6	82.3(1)	O5–Yb1–O6	82.4(2)
O5#1–Y1–O6	120.1(1)	O5#1–Er1–O6	119.6(1)	O5#1–Yb1–O6	120.9(2)
O1–Y1–O6	81.4(1)	O4#2–Er1–O6	81.6(1)	O4#2–Yb1–O6	82.0(2)
O3#2–Y1–O6	157.1(1)	O1–Er1–O6	157.4(1)	O1–Yb1–O6	156.2(2)
O4#3–Y1–O6	85.8(1)	O2#3–Er1–O6	86.5(1)	O2#3–Yb1–O6	86.1(2)
O5–Y1–N2#3	138.9(1)	O5–Er1–N2#3	138.8(1)	O5–Yb1–N2#3	139.3(2)
O5#1–Y1–N2#3	151.3(1)	O5#1–Er1–N2#3	151.2(1)	O5#1–Yb1–N2#3	151.1(2)
O1–Y1–N2#3	78.7(1)	O4#2–Er1–N2#3	78.2(1)	O4#2–Yb1–N2#3	78.0(2)
O3#2–Y1–N2#3	79.4(1)	O1–Er1–N2#3	79.6(1)	O1–Yb1–N2#3	79.3(2)
O4#3–Y1–N2#3	64.9(1)	O2#3–Er1–N2#3	65.6(1)	O2#3–Yb1–N2#3	65.9(2)
O6–Y1–N2#3	78.0(1)	O6–Er1–N2#3	78.3(1)	O6–Yb1–N2#3	77.3(2)

[a] Symmetry operations: #1 $–x + 2, –y + 2, –z$; #2 $–x + 2, –y + 1, –z$; #3 $x + 1/2, –y + 3/2, z + 1/2$. [b] Symmetry operations: #1 $–x + 1/2, –y + 5/2, –z + 1$; #2 $–x + 1/2, –y + 3/2, –z + 1$; #3 $–x + 1/2, y + 1/2, –z + 1/2$.

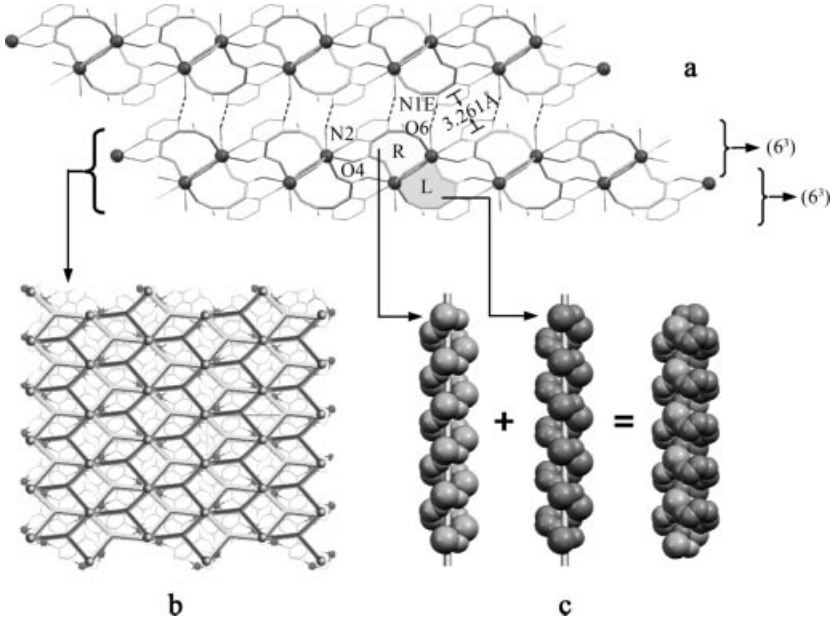

Figure 2. (a) 2D crystal packing diagram along the *b* axis for complex **1** showing interlayer interactions (hydrogen bonds indicated by dashed lines and π–π interactions by arrows and helical chains. (b) Topological representation of complex **1** down the *c* axis. (c) Space-filling model showing the helices constituted from two homochiral chains.

rality of the helices is in the RLLR mode in one layer as shown in Figure 2a. The same chiral helices are linked together through the remaining N2 and O4 atoms of the pza ligands, while two helical chains with opposite chirality are united directly at the metal nodes. This phenomenon may indicate that the twisted conformation of the ligand can effectively transfer the chiral information between the helices. However, packing these helical chains into a chiral solid still remains a challenge, which requires a deeper understanding of the role that the ligand has in the delivery of chirality and the crystal packing.

Table 2. Crystallographic data of **1**, **2** and **3**.

	1	**2**	**3**
Empirical formula	$C_6H_5N_2O_6Y$	$C_6H_5N_2O_6Er$	$C_6H_5N_2O_6Yb$
F_w	290.03	368.39	374.16
T /K	294(2)	294(2)	294(2)
Wavelength /Å	0.71073	0.71073	0.71073
Crystal system	Monoclinic	Monoclinic	Monoclinic
Space group	*C*2/*c*	*C*2/*c*	*C*2/*c*
a /Å	22.593(9)	22.514(5)	22.522(4)
b /Å	6.1250(19)	6.0984(12)	6.1128(12)
c /Å	17.960(7)	15.048(3)	14.998(3)
α /°	90	90	90
β /°	138.199(5)	127.760(3)	127.473(2)
γ /°	90	90	90
V /Å^3	1656.6(1)	1633.5(6)	1638.7(5)
Z	8	8	8
D_c /g cm^{-3}	2.326	3.004	3.033
μ /mm^{-1}	7.054	10.288	11.427
Reflections collected, unique, Rint	6121, 1963, 0.0443	5773, 1864, 0.0374	3851, 1424, 0.0657
R indices [$I>2\sigma(I)$]	R_1 = 0.0302, wR_2 = 0.0670	R_1 = 0.0284, wR_2 = 0.0491	R_1 = 0.0319, wR_2 = 0.0677
R indices (all data)	R_1 = 0.0403, wR_2 = 0.0702	R_1 = 0.0358, wR_2 = 0.0517	R_1 = 0.0470, wR_2 = 0.0769

Complexes **2** and **3** are isomorphous, and their structures are similar to complex **1** (see Table 1 and Table 2), except that complex **1** has a nearly 3-Å larger *c* value and a 10° larger *β* value than those of complexes **2** and **3**.

Upconversion Properties

In Figure 3 we can see a green emission band in the range 520–550 nm and a weaker red emission at 650–660 nm, which correspond to the transitions $^4S_{3/2}/^2H_{11/2}\rightarrow{}^4I_{15/2}$ and $^4F_{9/2}\rightarrow{}^4I_{15/2}$ respectively, for the codoped complex [(Y: Er, Yb)(pza)(OH)(H_2O)]$_n$ upon excitation at 975 nm.

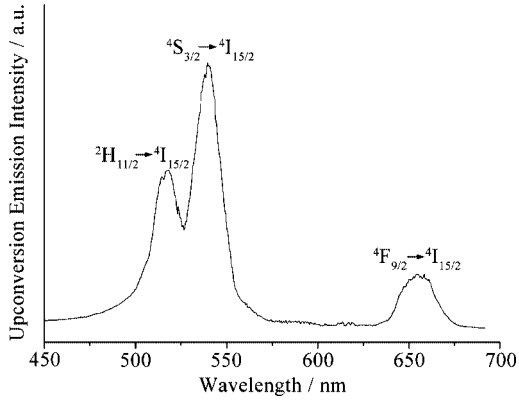

Figure 3. Upconversion emission for the Er^{III} ion in the Y: Er, Yb codoped coordination polymer.

Figure 4 shows the energy levels and upconversion mechanism in the Y: Er, Yb codoped coordination polymer. The Yb^{III} ion was excited by a 975 nm photon from the $^2F_{7/2}$ level to the excited $^2F_{5/2}$ state first. Then the energy was transferred from Yb^{III} to Er^{III} to pump the Er^{III} ion

from the $^4I_{15/2}$ state to the $^4I_{11/2}$ state. The Er^{III} ion, populated at the $^4I_{11/2}$ level, may transit to the $^4F_{7/2}$ state by a second-photon promotion. The $^4S_{3/2}$ and $^2H_{11/2}$ states can be populated by nonradiative relaxations from the $^4F_{7/2}$ state in the form of thermal vibration carried by phonons of ca. 2100 cm^{-1} (1620 cm^{-1} + 476 cm^{-1} in the IR spectrum) and 1400 cm^{-1} (1398 cm^{-1} in IR spectrum), respectively. The Er^{III} ions in the $^4S_{3/2}$ and $^2H_{11/2}$ states emit in the green range (518 and 540 nm) when going back to the ground state $^4I_{15/2}$.

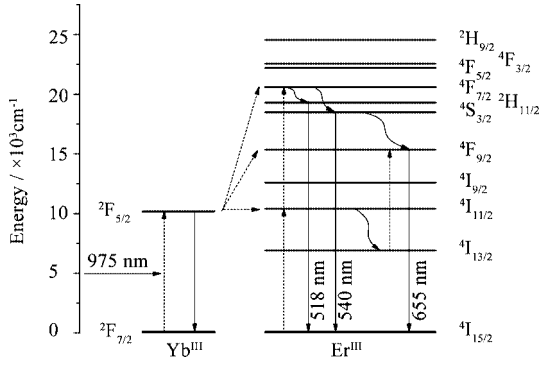

Figure 4. Energy-level diagram for the upconversion mechanism of the Y: Er, Yb codoped coordination polymer with excitation at 975 nm.

The red emission centred at 650 nm is generated by the $^4F_{9/2}$ to $^4I_{15/2}$ transition. There exist two possible routes for this process. The $^4F_{9/2}$ level can be reached by the nonradiative decay from the upper level, $^4S_{3/2}$.[11] However, the green emission ($^4S_{3/2}\rightarrow{}^4I_{15/2}$) was the strongest peak in our system, so this is not the main channel to the $^4F_{9/2}$ level. In the second possible route, Er^{III} ions in the $^4I_{11/2}$ state lose their energy in going to the $^4I_{13/2}$ level with some nonradiative decay involved. There is an energy gap of ca. 3500 cm^{-1} between the two states. The high-energy vibrations from the O–H group make the relaxation ($^4I_{11/2}\rightarrow{}^4I_{13/2}$) much more probable in this system. Then, a second photon energy (975 nm) pumps the Er^{III} from the $^4I_{13/2}$ to the $^4F_{9/2}$ level, and thus the red emission is obtained (see Figure 4).

Magnetic Properties

We investigated the magnetic properties of complexes **2** and **3** in the solid state at 2 kOe within the temperature range 2–300 K (Figure 5). For **2**, the observed value of $\chi_M T$ per [Er] unit is 12.22 $cm^3\,K\,mol^{-1}$ at room temperature (Figure 5a), which is slightly higher than the value expected for a free Er^{III} ion (11.48 $cm^3\,K\,mol^{-1}$).[12] Upon cooling, the value of $\chi_M T$ increases up to a maximum of 13.90 $cm^3\,K\,mol^{-1}$ at ca. 45 K and then abruptly decreases to reach 4.51 $cm^3\,K\,mol^{-1}$ at 2 K. The plot of χ_M^{-1} vs. T over the temperature range 50–300 K obeys the Curie–Weiss law [$\chi = C/(T - \theta)$] with C = 1.20 $cm^3\,K\,mol^{-1}$ and θ = 1.00 K. All of these results indicate that there is a ferromagnetic coupling between the Er^{III} ions. For **3**, the observed value of $\chi_M T$ per [Yb] unit is 2.47 $cm^3\,K\,mol^{-1}$ at room temperature (Figure 5b), which is close to the calculated value (2.57 $cm^3\,K\,mol^{-1}$) for a free Yb^{III} ion.[12] The value of $\chi_M T$ decreases slowly as the temperature decreases, to reach a value of 1.91 emu K mol^{-1} at 2 K. The plot of χ_M^{-1} vs. T over the temperature range 50–300 K obeys the Curie–Weiss law with C = 2.60 $cm^3\,K\,mol^{-1}$, θ = –17.13 K. The decrease in $\chi_M T$ and the negative value of θ are due primarily to the depopulation of the Stark levels of the Yb^{III} ion together with the possible weak antiferromagnetic coupling between the Yb^{III} ions, considering a possible interaction path through hydroxy bridges with a Yb···Yb distance of 3.601 Å.

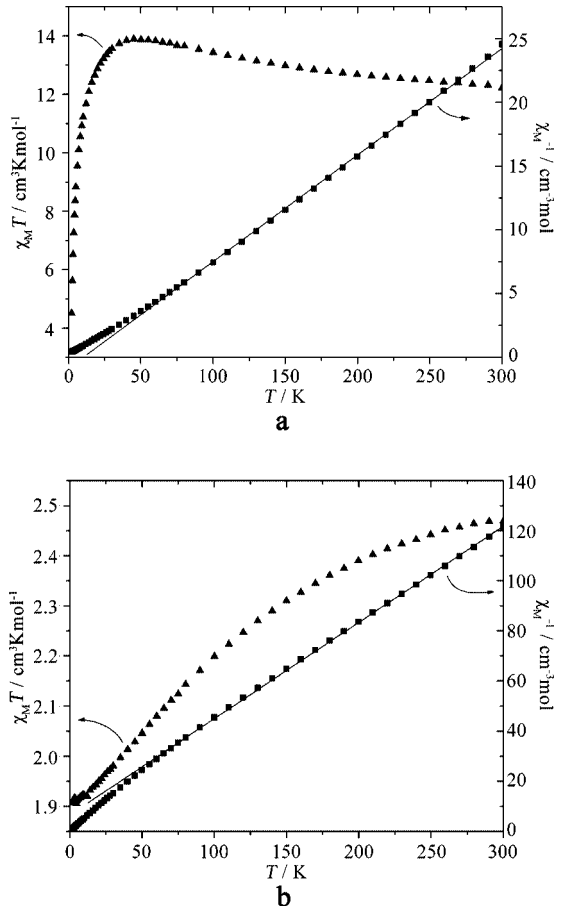

Figure 5. Plots of the temperature dependences of χ_M^{-1} (■) and $\chi_M T$ (▲) for complexes **2** (a) and **3** (b).

Conclusions

Three new lanthanide–organic frameworks with unusual $(4^3)_2(4^6,6^6,8^3)$ topology were synthesized under hydrothermal conditions. The arrangement of the helices in one layer in **1**–**3** shows that the twisted conformation of the ligand can effectively transfer the chiral information between the helices. The codoped coordination polymer [(Y: Er, Yb)(pza)(OH)(H_2O)]$_n$ emits green and red fluorescence by two-photon excitation. In addition, complex **2** shows a ferromagnetic coupling between the Er^{III} ions.

Experimental Section

General: All reagents were commercially available and were used without further purification. Elemental analyses of C, H and N were performed with an Elementar Vario EL analyzer. The IR spectra were recorded with a Nicolet Avatar 360 FTIR spectrometer by using the KBr pellet technique. The inductively coupled plasma (ICP) analysis was performed with a JY ULTIMA spectrometer. The upconversion luminescence spectra were measured by using a fluorescence spectrophotometer with a double-grating monochromator (JY-ISA, Fluorolog-Tau-3). A 975 nm continuous diode laser was used as the pump source. The direction of observation of the fluorescence was perpendicular to the direction of propagation of the pumping laser. Only the fluorescence emitted from the front surface of the samples was collected. The experimental conditions were held unchanged so as to ensure that the measurements for all the samples were comparable. The magnetic susceptibilities were obtained on crystalline samples with a Quantum Design MPMS XL-7 SQUID magnetometer. The experimental susceptibilities were corrected for contributions from the sample holder and the diamagnetism estimated from Pascal's constants.

$[Y(pza)(OH)(H_2O)]_n$ (1): The mixture of $YCl_3{\cdot}6H_2O$ (0.030 g, 0.1 mmol), 2,3-pyrazinedicarboxylic acid (0.017 g, 0.1 mmol), H_2O (5 mL) and aqueous NaOH (0.3 mL, 0.65 mol L^{-1}) was sealed in a 25-mL stainless steel reactor with a Teflon liner and heated at 190 °C for 72 h. Colourless plate-like crystals of **1** were obtained and washed with water. Yield: 0.020 g (68.96%). $C_6H_5N_2O_6Y$ (290.03): calcd. C 24.85, H 1.74, N 9.66; found C 24.70, H 1.97, N 9.54. IR (KBr): $\tilde{\nu}$ = 3405 (s), 1643 (vs), 1620 (vs), 1566 (m), 1448 (s), 1398 (s), 1360 (s), 1119 (m), 847 (m), 475 (m), 439 (m), 408 (m) cm^{-1}.

$[Er(pza)(OH)(H_2O)]_n$ (2): This compound was prepared by following the procedure for **1** but using $ErCl_3{\cdot}6H_2O$ instead of $YCl_3{\cdot}6H_2O$. Pink plate-like crystals of **2** were obtained. Yield: 0.019 g (51.58%). $C_6H_5ErN_2O_6$ (368.39): calcd. C 19.56, H 1.37, N 7.60; found C 19.53, H 1.59, N 7.61. IR (KBr): $\tilde{\nu}$ = 3399 (s), 1643 (vs), 1619 (vs), 1567 (m), 1448 (s), 1396 (s), 1363 (s), 1119 (m), 847 (m), 473 (m), 439 (m), 406 (m) cm^{-1}.

$[Yb(pza)(OH)(H_2O)]_n$ (3): This compound was prepared by following the procedure for **1** but using $Yb(NO_3)_3{\cdot}6H_2O$ instead of $YCl_3{\cdot}6H_2O$. Colourless plate-like crystals of **3** were obtained. Yield: 0.022 g (58.80%). $C_6H_5N_2O_6Yb$ (374.16): calcd. C 19.26, H 1.35, N 7.49; found C 19.17, H 1.35, N 7.34. IR (KBr): $\tilde{\nu}$ = 3406 (s), 1645 (vs), 1620 (vs), 1568 (m), 1450 (s), 1399 (s), 1363 (s), 1120 (m), 848 (m), 477 (m), 443 (m), 401 (m) cm^{-1}.

$[(Y: Er, Yb)(pza)(OH)(H_2O)]_n$: The codoped compounds were prepared by following the procedure for **1** but using $YCl_3{\cdot}6H_2O$, $ErCl_3{\cdot}6H_2O$ and $Yb(NO_3)_3{\cdot}6H_2O$ (for example, molar ratio: 92.0:4.0:4.0%) instead of 100% $YCl_3{\cdot}6H_2O$. Colourless plate-like crystals were obtained. Yield: 0.018 g (70.17%). $C_6H_5N_2O_6$(Y: Er, Yb) (296.53): calcd. C 24.30, H 1.82, N 9.45; found C 24.42, H 1.93, N9.33. IR (KBr): $\tilde{\nu}$ = 3404 (s), 1646 (vs), 1620 (vs), 1567 (m), 1449 (s), 1398 (s), 1363 (s), 1119 (m), 848 (m), 476 (m), 440 (m), 408 (m) cm^{-1}. ICP analysis showed that the molar ratio of Y/Er/Yb was 90.9:4.5:4.6 (%) in the product.

X-ray Structure Determination: Intensity data for **1**, **2** and **3** were collected at 294 K with a Bruker SMART 1000 CCD area detector diffractometer, using graphite-monochromated Mo-K_α radiation (λ = 0.71073 Å) in ϕ and ω scan modes, θ ranges 2.7° to 27.9° for **1**, 2.29° to 27.51° for **2**, 2.28° to 26.34° for **3**. Semiempirical absorption corrections were applied by using the SADABS program.[13] The structures were solved by direct methods[14] and refined by full-matrix least-squares on F^2 by using the programs SHELXS 97 and SHELXL 97, respectively.[14,15] All non-hydrogen atoms were refined anisotropically. The hydrogen atoms attached to the bridging hydroxy and the coordinated water molecules of **1**, **2** and **3** were located from the difference Fourier map. The other hydrogen atoms were generated geometrically and treated by a mixture of independent and constrained refinements. Details of crystallographic data of **1**, **2** and **3** are summarized in Table 2. CCDC 635120–635122 contain the supplementary crystallographic data for this paper. These data can be obtained free of charge from the Cambridge Crystallographic Data Centre via www.ccdc.cam.ac.uk/datarequest/cif.

Acknowledgments

We acknowledge the support from the National Natural Science Foundation of China (20331010, 20501003) and thank Prof. V. A. Blatov for help with the solution of the structure.

[1] a) U. Mueller, M. Schubert, F. Teich, H. Puetter, K. Schierle-Arndt, J. Pastré, *J. Mater. Chem.* **2006**, *16*, 626–636; b) C. J. Kepert, *Chem. Commun.* **2006**, 695–700; c) S. Kitagawa, S. I. Noro, T. Nakamura, *Chem. Commun.* **2006**, 701–707; d) N. R. Champness, *Dalton Trans.* **2006**, 877–880; e) J. D. Wuest, *Chem. Commun.* **2005**, 5830–5837; f) D. Bradshaw, J. B. Claridge, E. J. Cussen, T. J. Prior, M. J. Rosseinsky, *Acc. Chem. Res.* **2005**, *38*, 273–282; g) B. Kesanli, W. B. Lin, *Coord. Chem. Rev.* **2003**, *246*, 305–326.

[2] a) H. L. Sun, B. Q. Ma, S. Gao, S. R. Batten, *Cryst. Growth Des.* **2006**, *6*, 1261–1263; b) J. F. Eubank, R. D. Walsh, P. Poddar, H. Srikanth, R. W. Larsen, M. Eddaoudi, *Cryst. Growth Des.* **2006**, *6*, 1453–1457; c) B. Gómez-Lor, E. Gutiérrez-Puebla, M. Iglesias, M. A. Monge, C. Ruiz-Valero, N. Snejko, *Chem. Mater.* **2005**, *17*, 2568–2573; d) L. Chen, X. H. Bu, *Inorg. Chem.* **2006**, *45*, 4654–4660; e) S. Q. Zang, Y. Su, Y. Z. Li, Z. P. Ni, H. Z. Zhu, Q. J. Meng, *Inorg. Chem.* **2006**, *45*, 3855–3857; f) Y. Q. Sun, J. Zhang, Y. M. Chen, G. Y. Yang, *Angew. Chem. Int. Ed.* **2005**, *44*, 5814–5817; g) L. Han, M. C. Hong, *Inorg. Chem. Commun.* **2005**, *8*, 406–419; h) B. Zhai, L. Yi, H. S. Wang, B. Zhao, P. Cheng, D. Z. Liao, S. P. Yan, *Inorg. Chem.* **2006**, *45*, 8471–8473.

[3] a) X. B. Zhao, B. Xiao, A. J. Fletcher, K. M. Thomas, D. Bradshaw, M. J. Rosseinsky, *Science* **2004**, *306*, 1012–1015; b) S. Kitagawa, R. Kitaura, S. I. Noro, *Angew. Chem. Int. Ed.* **2004**, *43*, 2334–2375; c) G. Férey, C. Mellot-Draznieks, C. Serre, F. Millange, *Acc. Chem. Res.* **2005**, *38*, 217–225; d) J. L. C. Rowsell, O. M. Yaghi, *Angew. Chem. Int. Ed.* **2005**, *44*, 4670–4679; e) M. Latroche, S. Surblé, C. Serre, C. Mellot-Draznieks, P. L. Llewellyn, J. H. Lee, J. S. Chang, S. H. Jhung, G. Férey, *Angew. Chem. Int. Ed.* **2006**, *45*, 8227–8231; f) S. M. Humphrey, J. S. Chang, S. H. Jhung, J. W. Yoon, P. T. Wood, *Angew. Chem. Int. Ed.* **2007**, *46*, 272–275.

[4] a) T. Ezuhara, K. Endo, Y. Aoyama, *J. Am. Chem. Soc.* **1999**, *121*, 3279–3283; b) Y. Xu, L. Han, Z. Z. Lin, C. P. Liu, D. Q. Yuan, Y. F. Zhou, M. C. Hong, *Eur. J. Inorg. Chem.* **2004**, 4457–4462; c) P. A. Maggard, C. L. Stern, K. R. Poeppelmeier, *J. Am. Chem. Soc.* **2001**, *123*, 7742–7743; d) M. H. Zeng, B. Wang, X. Y. Wang, W. X. Zhang, X. M. Chen, S. Gao, *Inorg. Chem.* **2006**, *45*, 7069–7076; e) C. D. Wu, A. G. Hu, L. Zhang, W. B. Lin, *J. Am. Chem. Soc.* **2005**, *127*, 8940–8941.

[5] a) J. Wu, Y. L. Song, E. P. Zhang, H. W. Hou, Y. T. Fan, Y. Zhu, *Chem. Eur. J.* **2006**, *12*, 5823–5831; b) K. Liang, H. G. Zheng, Y. L. Song, M. F. Lappert, Y. Z. Li, X. Q. Xin, Z. X. Huang, J. T. Chen, S. F. Lu, *Angew. Chem. Int. Ed.* **2004**, *43*, 5776–5779.

[6] a) T. Glaser, M. Heidemeier, T. Weyhermüller, R. D. Hoffmann, H. Rupp, P. Müller, *Angew. Chem. Int. Ed.* **2006**,

45, 6033–6037; b) U. García-Couceiro, O. Castillo, A. Luque, J. P. García-Terán, G. Beobide, P. Román, *Cryst. Growth Des.* **2006**, *6*, 1839–1847; c) X. T. Liu, X. Y. Wang, W. X. Zhang, P. Cui, S. Gao, *Adv. Mater.* **2006**, *18*, 2852–2856; d) Y. Z. Zhang, Z. M. Wang, S. Gao, *Inorg. Chem.* **2006**, *45*, 5447–5454; e) Y. Z. Zheng, M. L. Tong, W. X. Zhang, X. M. Chen, *Angew. Chem. Int. Ed.* **2006**, *45*, 6310–6314.

[7] a) D. Bradshaw, T. J. Prior, E. J. Cussen, J. B. Claridge, M. J. Rosseinsky, *J. Am. Chem. Soc.* **2004**, *126*, 6106–6114; b) W. Gerhardt, M. Črne, M. Weck, *Chem. Eur. J.* **2004**, *10*, 6212–6221; c) Q. R. Fang, G. S. Zhu, M. Xue, J. Y. Sun, F. X. Sun, S. L. Qiu, *Inorg. Chem.* **2006**, *45*, 3582–3587.

[8] a) A. de Bettencourt-Dias, *Inorg. Chem.* **2005**, *44*, 2734–2741; b) P. Lenaerts, K. Driesen, R. V. Deun, K. Binnemans, *Chem. Mater.* **2005**, *17*, 2148–2154; c) Z. H. Zhang, Y. Song, T. A. Okamura, Y. Hasegawa, W. Y. Sun, N. Ueyama, *Inorg. Chem.* **2006**, *45*, 2896–2902; d) A. Nag, P. J. Schmidt, W. Schnick, *Chem. Mater.* **2006**, *18*, 5738–5745; e) H. T. Zhang, Y. Song, Y. X. Li, J. L. Zuo, S. Gao, X. Z. You, *Eur. J. Inorg. Chem.* **2005**, 766–772.

[9] a) L. Luo, W. P. W. Lai, L. K. Wong, W. T. Wong, K. F. Li, K. W. Cheah, *Chem. Phys. Lett.* **2004**, *398*, 372–376; b) K. L. Wong, W. M. Kwok, W. T. Wong, D. L. Phillips, K. W. Cheah, *Angew. Chem. Int. Ed.* **2004**, *43*, 4659–4662; c) J. Yang, Q. Yue, G. D. Li, J. J. Gao, G. H. Li, J. S. Chen, *Inorg. Chem.* **2006**, *45*, 2857–2865; d) D. F. Weng, X. J. Zheng, L. P. Jin, *Eur. J. Inorg. Chem.* **2006**, 4184–4190.

[10] a) V. A. Blatov, A. P. Shevchenko, V. N. Serezhkin, *J. Appl. Crystallogr.* **2000**, *33*, 1193–1193; b) V. A. Blatov, L. Carlucci, G. Ciani, D. M. Proserpio, *CrystEngComm* **2004**, *6*, 377–395.

[11] G. S. Yi, B. Q. Sun, F. Z. Yang, D. P. Chen, Y. X. Zhou, J. Cheng, *Chem. Mater.* **2002**, *14*, 2910–2914.

[12] O. Kahn in *Molecular Magnetism*, VCH Publishers, New York, **1993**.

[13] G. M. Sheldrick, *SADABS*, Program for Empirical Absorption Correction of Area Detector Data, University of Göttingen, Göttingen, Germanny, **1997**.

[14] G. M. Sheldrick, *SHELXS 97*, Program for Crystal Structure Solution, University of Göttingen, Göttingen, Germanny, **1997**.

[15] G. M. Sheldrick, *SHELXL 97*, Program for Crystal Structure Refinement, University of Göttingen, Göttingen, Germanny, **1997**.

Received: January 31, 2007
Published Online: June 1, 2007

